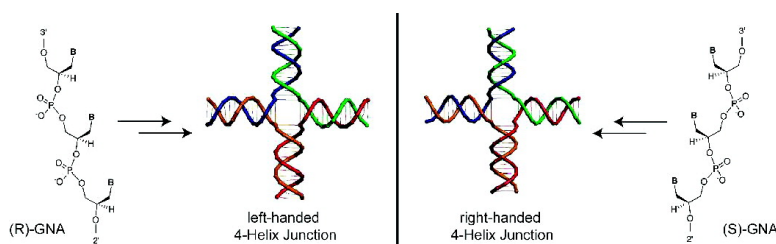


Synthesis of Two Mirror Image 4-Helix Junctions Derived from Glycerol Nucleic Acid

Richard S. Zhang, Elizabeth O. McCullum, and John C. Chaput

J. Am. Chem. Soc., **2008**, 130 (18), 5846-5847 • DOI: 10.1021/ja800079j • Publication Date (Web): 12 April 2008

Downloaded from <http://pubs.acs.org> on February 8, 2009



More About This Article

Additional resources and features associated with this article are available within the HTML version:

- Supporting Information
- Links to the 1 articles that cite this article, as of the time of this article download
- Access to high resolution figures
- Links to articles and content related to this article
- Copyright permission to reproduce figures and/or text from this article

[View the Full Text HTML](#)

Synthesis of Two Mirror Image 4-Helix Junctions Derived from Glycerol Nucleic Acid

Richard S. Zhang, Elizabeth O. McCullum, and John C. Chaput*

Center for BioOptical Nanotechnology, The Biodesign Institute, and Department of Chemistry and Biochemistry, Arizona State University, Tempe, Arizona 85287-1604

Received January 4, 2008; E-mail: john.chaput@asu.edu

Structural DNA nanotechnology uses sequence minimization rules to construct micrometer scale objects with nanometer scale features.¹ This is a “bottom-up” approach to nanotechnology that relies on Watson–Crick base pairing to assemble DNA motifs into different geometric shapes and patterns.² While substantial effort has been devoted to expanding the programmability of standard B-form DNA,³ considerably less attention has been given to the development of unnatural DNA nanostructures.⁴ By expanding DNA nanotechnology to include alternative polymers, it should be possible to create nanostructures with chemical and physical properties not found in natural DNA.⁵ Toward this goal, it would be useful to have a genetic system that was capable of forming nanostructures independent of DNA or RNA hybridization. Of the known orthogonal genetic systems,⁶ only glycerol nucleic acid (GNA) provides easy access to both left- and right-handed helical geometries.⁷ This unusual feature suggests that GNA could be used to construct nanostructures with unique topologies. Here, we wish to report the first synthesis of a nanostructure (Figure 1) based entirely on GNA self-pairing—two 4-helix junctions (4HJ) with mirror image symmetry.

Using established methodology,^{7,8} we synthesized all four phosphoramidite monomers of (*R*)- and (*S*)-GNA. The monomers were used as building blocks to construct mixed sequence oligonucleotides of (*R*)- and (*S*)-GNA. To prevent unwanted base-catalyzed decomposition during the deprotection step, we capped each GNA strand at both ends with a single deoxyribonucleotide.⁹ The sequence for each strand (Figure 2A) was chosen based on a previous design by Seeman and co-workers, where DNA was used to assemble a synthetic 4HJ.¹⁰ In contrast to natural 4HJs, which undergo branch migration due to regions of symmetry within their sequence, synthetic 4HJs are designed to be immobile structures.¹¹ Using our GNA oligonucleotides, we aimed to determine how well the sequence optimization strategies used for DNA nanotechnology would apply to GNA, and whether GNA could be used as a molecular scaffold for assembling nanostructures with left- and right-handed helical geometries.

We began using nondenaturing gel electrophoresis to study the propensity for GNA to self-assemble into an immobile 4HJ. In this assay, DNA complexes are separated based on size and charge, with higher molecular weight complexes having a slower electrophoretic mobility than smaller complexes. On the basis of the design (Figure 2A), the desired 4HJ should result when GNA strands 1–4 are present in equimolar ratios in solution. To identify the intermediate forms of the 4HJ, we separately annealed strand 1 with strands 2, 2 + 3, and 2 + 3 + 4 and analyzed the samples by nondenaturing gel electrophoresis. Our initial attempt at visualizing the gel by ethidium

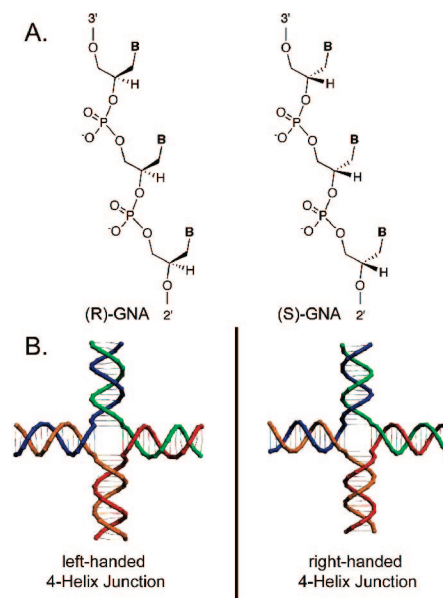


Figure 1. An immobile 4-helix junction composed of glycerol nucleic acid. (A) Chemical structure of (*R*)- and (*S*)-GNA. (B) Cartoon image of left- and right-handed 4-helix junctions.

bromide or SYBR-Gold staining methods failed to detect the presence of any GNA. Since this limitation could be due to structural differences between GNA and natural DNA and RNA, we decided to enzymatically radiolabel the DNA residue at the 3'-end of each GNA strand with P³²-ATP. To our surprise, the chimeric GNA strands proved to be remarkably good substrates for T4 polynucleotide kinase. Using P³²-labeled GNA, we then repeated the strand-mixing assay and imaged the gel by phosphorimaging. The resulting image (Figure 2A) shows that when adjacent strands are added to the mixture higher order complexes emerge that exhibit mobility shifts consistent with the formation of the dimer and trimer intermediates and final tetramer product of the 4HJ. The same result was observed using (*R*)- and (*S*)-GNA and natural DNA (Supporting Information). We verified that all four strands associate in the 4HJ by comparing the gel mobility of each monomer, dimer, and trimer strand combination (Supporting Information).¹⁰ Complete formation of the tetramer structure demonstrates that GNA is capable of forming simple nucleic acid nanostructures.

Next, we used circular dichroism (CD) spectroscopy to examine the structural properties of our GNA nanostructures. The CD spectra of both 4HJs are given in Figure 2B. The two nanostructures exhibit mirror image symmetry with strong CD signals at 224 and 280 nm. This result is consistent with previous CD data collected on double-stranded GNA duplexes^{7a} and supports the formation

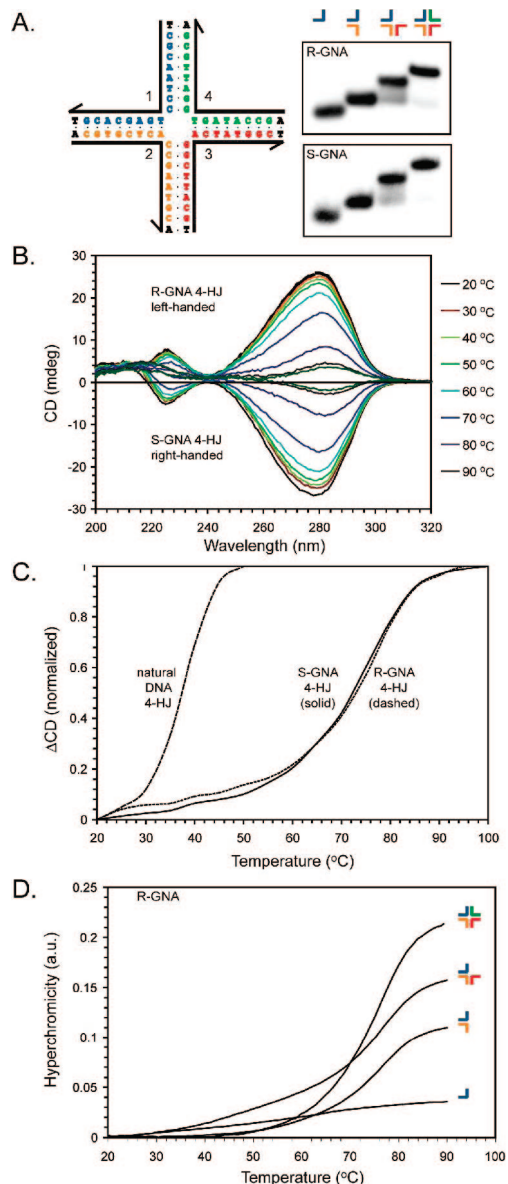


Figure 2. Characterization of two GNA 4-helix junctions. (A) The design used to assemble the GNA 4HJ (left). Nondenaturing gel electrophoresis mobility shift assays showing the monomer, dimer, trimer, and tetramer forms of the 4HJ (right). Drawn above each lane is a schematic view of the resulting complex. (B) CD analysis of the 4HJs derived from (*R*)- and (*S*)-GNA. (C and D) Thermal denaturing curves obtained from temperature-dependent CD and UV absorbance indicate that GNA forms a closed 4HJ that is thermally superior to the analogous DNA nanostructure.

of short helices in each arm of the 4HJ. The CD spectra for both GNA nanostructures differ considerably from natural DNA and RNA, indicating that GNA likely adopts a unique helical structure. This hypothesis is supported by the observation that GNA cross-pairs weakly with RNA but not all with DNA.⁷ Analysis of the CD spectra at different temperatures revealed a Cotton effect that decreases with increasing temperature, as expected for a self-assembled complex with a melting transition.

Last, we examined the thermal stability of the GNA 4HJ using temperature-dependent spectroscopy. Quantitative values for the thermal stability of the 4HJs were obtained by monitoring the change in the CD signal at 280 nm as a function of increasing temperature. As illustrated in Figure 2C, 4HJs constructed from (*R*)- and (*S*)-GNA gave nearly identical curves with a single transition between the folded and denatured states. The data from

both melting experiments were fit to a standard sigmoidal curve, which gave a T_m of 76 °C for the two GNA structures. Comparison of the hyperchromicity (Figure 2D) obtained for UV melts on strands 1, 1 + 2, 1 + 2 + 3, and 1 + 2 + 3 + 4 reveals a stepwise increase in absorbance consistent with a closed 4HJ.¹⁰

To compare the thermal stability of a 4HJ constructed of GNA to one constructed of DNA, we repeated the thermal denaturation experiment using DNA oligonucleotides of identical sequence. As expected, the DNA version of the 4HJ (Figure 2C) gave a melting transition of 37 °C, which is consistent with the denaturing plot given in the original description of the 4HJ by Seeman.¹⁰ On the basis of these data, it appears that the GNA 4HJ is significantly more stable than the DNA 4HJ. This is a remarkable achievement given that the GNA backbone is acyclic and one atom shorter than the backbone found in DNA and RNA. In the absence of detailed structural information, it is difficult to rationalize the extreme thermal stability of GNA. One possibility is that the flexible nature of the acyclic backbone allows GNA to access base pairing and base stacking interactions that are optimal for two complementary strands. DNA and RNA, though optimal in many other ways, would then have pairing interactions that are weaker due to structural constraints imposed by the furanose ring.

In summary, we describe the use of glycerol nucleic acid as a simple building block for assembling nucleic acid nanostructures with left- and right-handed helical geometries. We suggest that GNA could be used as a general method for constructing chiral nanostructures with unique topologies and extreme thermal stabilities. Once the helical dimensions of GNA are known, we predict that the sequence optimization methods used to program DNA will also apply to GNA since both polymers self-assemble using the same Watson–Crick base pairing rules. The current study therefore represents a first step toward the development of unnatural nucleic acid nanostructures.

Acknowledgment. This work was supported by grants from the Biodesign Institute to J.C.C. We wish to thank Hao Yan for helpful comments and suggestions.

Supporting Information Available: Detailed protocols, gel electrophoresis, and CD spectroscopy data. This material is available free of charge via the Internet at <http://pubs.acs.org>.

References

- Seeman, N. C. *J. Theor. Biol.* **1982**, *99*, 237–247.
- For review, see: (a) Lin, C.; Liu, Y.; Rinker, S.; Yan, H. *ChemPhysChem* **2006**, *7*, 1641–1647. (b) Seeman, N. C. *Trends Biochem. Sci.* **2005**, *30*, 119–125. (c) Niemeyer, C. M. *Curr. Opin. Chem. Biol.* **2000**, *4*, 609–618. (d) Seeman, N. C. *Annu. Rev. Biophys. Biomol. Struct.* **1998**, *27*, 225–248.
- (a) Seeman, N. C. *Chem. Biol.* **2003**, *10*, 1151–1159. (b) Feldkamp, U.; Niemeyer, C. M. *Angew. Chem., Int. Ed* **2006**, *45*, 1856–1876.
- Ng, P.-S.; Bergstrom, D. E. *Nano Lett.* **2005**, *5*, 107–111.
- For example, see: (a) Liu, H.; Gao, J.; Lynch, S. R.; Saito, Y. D.; Maynard, L.; Kool, E. T. *Science* **2003**, *302*, 868–871. (b) Chaput, J. C.; Switzer, C. *Proc. Natl. Acad. Sci. U.S.A.* **1999**, *96*, 10614–10619.
- (a) Eschenmoser, A. *Science* **1999**, *284*, 2118–2124. (b) Schoning, K.-U.; Scholz, P.; Guntha, S.; Wu, X.; Krishnamurthy, R.; Eschenmoser, A. *Science* **2000**, *290*, 1347–1351.
- (a) Zhang, L.; Peritz, A.; Meggers, E. *J. Am. Chem. Soc.* **2005**, *127*, 4174–4175. (b) Yang, Y.-W.; Zhang, S.; McCullum, E. O.; Chaput, J. C. *J. Mol. Evol.* **2007**, *65*, 289–295.
- (a) Schlegel, M. K.; Peritz, A. E.; Kittigowittana, K.; Zhang, L.; Meggers, E. *ChemBioChem* **2007**, *8*, 927–932. (b) Acevedo, O. L.; Andrews, R. S. *Tetrahedron Lett.* **1996**, *37*, 3931–3139. (c) Holy, A. *Collect. Czech. Chem. Commun.* **1975**, *40*, 187–214. (d) Zhang, L.; Peritz, A. E.; Meggers, E. *Synthesis* **2006**, 645–653.
- Tsai, C.-H.; Chen, J.; Szostak, J. W. *Proc. Natl. Acad. Sci. U.S.A.* **2007**, *104*, 14598–14603.
- Kallenbach, N. R.; Ma, R.-I.; Seeman, N. C. *Nature* **1983**, *305*, 829–831.
- Holliday, R. *Genet. Res.* **1964**, *5*, 282–304.

JA800079J